Acta Biomaterialia 6 (2010) 2227–2236

Contents lists available at ScienceDirect

Acta Biomaterialia

journal homepage: www.elsevier.com/locate/actabiomat

In vivo bone response and mechanical evaluation of electrosprayed CaP nanoparticle coatings using the iliac crest of goats as an implantation model

Corinne Schouten [a], Gert J. Meijer [a,b,*], Jeroen J.J.P. van den Beucken [a], Sander C.G. Leeuwenburgh [a], Lise T. de Jonge [a], Joop G.C. Wolke [a], Paul H.M. Spauwen [c], John A. Jansen [a]

[a] Department of Biomaterials, Radboud University Nijmegen Medical Center, Nijmegen, The Netherlands
[b] Department of Oral and Maxillofacial Surgery, Radboud University Nijmegen Medical Center, Nijmegen, The Netherlands
[c] Department of Plastic and Reconstructive Surgery, Radboud University Nijmegen Medical Center, Nijmegen, The Netherlands

ARTICLE INFO

Article history:
Received 9 September 2009
Received in revised form 20 November 2009
Accepted 23 November 2009
Available online 26 November 2009

Keywords:
Animal model
Calcium phosphate coating
Electrostatic spray deposition

ABSTRACT

Recent trends in clinical implantology include the use of endosseous dental implant surfaces embellished with nano-sized modifications. The current study was initiated to evaluate the mechanical properties, as well as the potential beneficial effects, of electrosprayed CaP nanoparticle-coated (nano-CaP) implants on the in vivo osteogenic response, compared with grit-blasted, acid-etched (GAE) implant surfaces as controls. For this purpose nano-CaP coatings were deposited on cylindrical screw-type (St) implants and implanted bilaterally into the iliac crest of goats for 6 weeks. In addition to histological and histomorphometrical analyses, insertion torque and removal torque values were measured on implant placement and retrieval, respectively. The present study showed similar insertion and removal torque values for nano-CaP-coated and GAE control implants, with no statistically significant increase in torque value during the implant period for either group. With regard to bone–implant contact and peri-implant bone volume, no significant differences were found between nano-CaP-coated and GAE implants after 6 weeks implantation. In conclusion, this study has demonstrated that in situations in which implants are placed in a non-compromised situation using a standard press fit implantation strategy the performance of electrosprayed nano-CaP coatings is comparable with GAE implants, both with respect to implant fixation and bone healing response.

1. Introduction

The long-term clinical success of orthopedic and dental implants is greatly influenced by their physicochemical surface characteristics, since the overall tissue response (i.e. adsorption of proteins, cell adhesion and spreading) responsible for optimal anchoring of the implant into the native bone tissue, takes place at the surface of the implant [1,2]. Consequently, research is increasingly focusing on the modification of implant surfaces to improve the properties of the bulk material and thereby enhance the biological healing response. These implant surface modifications can rely on either chemical or topographical alterations, or a combination thereof [3].

Various reports have already claimed a positive correlation between implant micro/nano surface roughness and interfacial strength, which can, for example, be measured by removal torque testing [4–6]. In addition, a faster rate and higher degree of bone formation has been reported for roughened surfaces [7–10]. Regarding surface chemistry, bioactive materials, such as calcium phosphate (CaP) ceramics, have routinely been applied as thin coatings onto metallic implant materials (mostly titanium, Ti), as these ceramics are too brittle for use as a bulk material under loaded conditions. The excellent biological properties of CaP ceramics can be exploited in combination with the mechanical strength of metallic materials in such coated implants [11–14].

Since the introduction of CaP coatings these ceramics have proved to be osteoconductive [15,16], to improve implant fixation [17], to increase bone–implant contact [18,19] and to facilitate the bridging of gaps up to 1.0 mm [20,21]. Various techniques have been used to deposit CaP coatings onto implant surfaces, of which plasma spraying is still the most widely used [14,22,23]. Despite positive results regarding the osteoconductive and bone bonding behavior of plasma-sprayed coatings [24,25], this deposition technique is only capable of producing coatings with a minimal thickness of 30 μm, thereby introducing the risk of coating delamination. Additionally, incorporation of organic biomolecules (e.g. growth factors) to further enhance the biological activity of CaP coatings has been hampered due to the extremely high temperatures during the plasma spray process. To overcome

* Corresponding author. Address: Department of Biomaterials 309, Radboud University Nijmegen Medical Center, P.O. Box 9101, 6500 HB Nijmegen, The Netherlands. Tel.: +31 24 3614006; fax: +31 24 3614657.
E-mail address: g.meijer@dent.umcn.nl (G.J. Meijer).

1742-7061/$ - see front matter © 2009 Acta Materialia Inc. Published by Elsevier Ltd. All rights reserved.
doi:10.1016/j.actbio.2009.11.030

this limitation the electrospraying of suspensions of nano-sized crystalline CaP particles was recently suggested, to enable the deposition of nanometer thin CaP films at low temperatures [26]. As in these suspensions CaP crystals have already been formed prior to spraying, high temperatures during coating deposition and additional heat treatments to crystallize the ceramic are bypassed. Moreover, nanometer thin coatings will reduce the risk of coating delamination related to the micrometer thick plasma-sprayed coatings. Also, from a biological point of view there is increasing interest in the use of CaP nanoparticles (nano-CaP) for orthopedic and dental applications, as they resemble the nano-crystalline nature of bone mineral, increase osteoblast adhesion [27] and improve osteogenic behavior [28]. To date, it has been shown that CaP particle size is directly related to the bioactive properties of CaP [29,30]. Although these results are promising, in vivo experiments are needed to obtain conclusive data on the capacity of nanometer thick electrosprayed CaP coatings to enhance the osteogenic response.

Consequently, the current study aimed at evaluating the mechanical properties and in vivo response of electrosprayed nano-CaP-coated implants using a goat implantation model. For this purpose, nano-CaP coatings were deposited onto cylindrical screw-type (St) implants and implanted bilaterally into the iliac crest of goats for 6 weeks. Grit-blasted, acid-etched (GAE) implants served as controls. Insertion and removal torque values were determined for the bone implants at implant placement and retrieval, respectively. Further, the osteogenic response was evaluated qualitatively (histology) and quantitatively (histomorphometry).

2. Materials and methods

2.1. Materials

Helix® dental implants, made of titanium alloy (Ti–6AL–4V), grit-blasted and acid-etched (GAE) to roughen the surface (roughness R_a = 1.3–1.4 μm), were provided by Dyna Dental Engineering BV (Bergen op Zoom, The Netherlands). These cylindrical St implants were based on a root shape core and a straight, self-tapping thread measuring 13 mm in length and 4.2 mm in diameter. Commercially available nano-CaP suspensions were acquired from Berkeley Advanced Biomaterials (Berkeley, CA).

2.2. Implant preparation and cleaning

Prior to coating deposition all St implants were cleaned ultrasonically in 10% nitric acid (15 min), acetone (15 min) and isopropanol (15 min) and thereafter air dried.

2.3. Coating deposition

For coating deposition at low temperatures nano-CaP suspensions containing nano-sized crystalline carbonate apatite particles were used, as reported previously [28]. Commercially available ethanol-based CaP suspensions (Berkeley Advanced Biomaterials) were diluted in 100% ethanol (10:90 vol.%) prior to electrospraying. To deposit the nano-CaP coatings a commercially available vertical electrostatic spray deposition set-up (Advanced Surface Technology, Bleiswijk, The Netherlands), as described by de Jonge et al. [31], was used. The St implants were coated in two runs (with turns of 180°) of 5 min each to obtain complete coverage. The standardized conditions were: 15% relative humidity; 40 °C substrate holder temperature; 40 mm nozzle to substrate distance; 0.15 ml h^{-1} liquid flow rate; 8–10.5 kV applied voltage.

2.4. Coating characterization

2.4.1. Coating thickness

The thickness of the deposited nano-CaP coating, corresponding to an electrospray deposition time of 5 min, was determined by atomic force microscopy (AFM) (Multimode Nanoscope IIIa) in an accurate model system using silicon wafers as substrate (unpublished results). Briefly, one half of the silicon wafers was coated with nano-CaP while the other half was left uncoated. Subsequently the wafers were scanned at the non-coated/coated boundary in tapping mode at a rate of ~1 Hz using 100 μm long silicon cantilevers (NSG10, NT-MDT) with average nominal resonant frequencies of 250 kHz, spring constants of 15 N m^{-1} and a tip radius of curvature of <10 nm. To analyze the height difference between the silicon wafer and the coating, which corresponds to the coating thickness, nanoscope imaging software (version 6.13rl, Veeco) was used.

2.4.2. Coating morphology

Scanning electron microscopy (SEM) (JEOL 6310, Tokyo, Japan) was performed to examine the surface morphology of the implants of both experimental groups (GAE and nano-CaP).

2.4.3. Coating surface roughness

Average surface roughness values (R_a) were determined for both experimental groups (GAE and nano-CaP) using a Universal Surface Tester (UST) (Innowep, Wurzburg, Germany).

2.4.4. Coating adhesion upon implant insertion in artificial bone

To evaluate adhesion of the nano-CaP coatings to the St implants biomedical test blocks (Sawbones®; Pacific Research Laboratories, Washington, DC) were used as an artificial bone model. These test blocks offer uniform and consistent mechanical properties that eliminate the variability encountered when using cadaver bones. The test blocks consisted of solid, rigid polyurethane foam with a density of 0.48 g cm^{-3} covered with a 1 mm thick fiber filled epoxy sheet, corresponding to human cancellous and cortical bone, respectively. In accordance with the manufacturer's recommendations, drill holes with a diameter of 4.0 mm were made in the test blocks using a dental drill (KaVo EWL Dental GmbH, Biberach, Germany) at a bit speed of 2000 r.p.m. under continuous cooling. Subsequently the St implants were installed. In order to prevent damage to the coating upon explantation by means of unscrewing the test blocks were cross-sectioned and the implants removed. In this way the test procedure closely resembles the clinical situation, in which implants are left in situ after installation. After explantation the implants were carefully brushed to remove adherent polyurethane foam fragments. Subsequently the nano-CaP coatings were thoroughly inspected using SEM. The amount of nano-CaP coating remaining on the implant surface was quantified using the ortho-cresolphthalein complexone (OCPC) method. In brief, the implants were incubated overnight in 1 ml of 0.5 N acetic acid on a shaker table. For analysis 300 μl of work reagent was added to aliquots of 10 μl of sample or standard in a 96-well plate. The plate was incubated for 10 min at room temperature, after which the plate was read at 570 nm. Serial dilutions of $CaCl_2$ (0–100 μg ml^{-1}) were used to produce a standard curve. As received nano-CaP-coated implants were used as controls.

2.5. Experimental animal groups

In the present study St implants were placed in the iliac crests of four goats. Two experimental groups were used: grit-blasted and acid-etched (GAE); GAE + nano-CaP. Sterility of the substrates was obtained by autoclaving.

2.6. Surgical procedure

Four healthy female Saanen goats with an average age of 26–30 months and a mean body weight of 50–60 kg were selected. All in vivo work was conducted in accordance with ISO standards and the protocols of the Radboud University Nijmegen Medical Center, Nijmegen, The Netherlands. National guidelines for care and use of laboratory animals were obeyed and the approval of the Radboud University Experimental Animal Ethical Committee was obtained (RUDEC 2008-189). The St implants were inserted into trabecular bone in the iliac crest, as described by Schouten et al. [32]. All animals received subcutaneous injections of the prophylactic antibiotic Albipen® to reduce the risk of peri-operative infection: 15% Albipen at 3 ml 50 kg^{-1} pre-operative and Albipen LA at 7.5 ml 50 kg^{-1} for 3 days post-operative (Intervet BV, Boxmeer, The Netherlands). Surgery was performed under general inhalation anesthesia and sterile conditions. Anesthesia was induced by an intravenous injection of Pentobarbital®, after which the goats were intubated and connected to an inhalation ventilator with a constant volume of a mixture of nitrous oxide, isoflurane and oxygen. After intubation the incision sites and surrounding areas were shaved, washed and disinfected with povidone–iodine.

For insertion of the St implants each animal was immobilized in a prone position. A transverse skin incision was made, starting at the intermediate zone of the iliac crest (i.e. half way between the posterior superior iliac spine and anterior superior iliac spine), subsequently processing towards the anterior superior iliac spine (i.e. from medial to lateral) on both sides of the vertebral column (Fig. 1). The incision was continued through the underlying tissue layers down to the periosteum. The periosteum was undercut and lifted aside, fully exposing the iliac crest. Subsequently cavities were created with a 2.0 mm pilot drill, which were gradually widened using drills of increasing size until a final diameter of 4.0 mm was reached. Drilling was performed using a dental bur (Elcomed 100, W&H Dental Werk Burmoos, Austria) at low rotational drill speeds (800–1200 r.p.m.) and continuous external cooling with saline solution. Four implant locations were created in each iliac wing, with an interimplant distance of about 1 cm (Fig. 1). After preparation the implant locations were irrigated and the implants inserted manually. For each iliac wing insertion torque values (torque-in) were measured for two implants using a MGT 50® digital torque gauge (MARK-10 Corp., New York). In total 32 St implants (16 implants per experimental group) were implanted into four goats. Following statistical randomization, the implants were clustered into groups of two implants (GAE vs. nano-CaP-coated). After implant placement the soft tissue layers and skin were closed with resorbable sutures (Vicryl® 4·0, Ethicon Products, Amersfoort, The Netherlands). To reduce post-operative pain, Finadyne® was administered for 2 days post-operatively. After 6 weeks implantation all four goats were euthanized with an overdose of Nembutal®.

2.7. Implant retrieval

Immediately after killing the animals the implants, with surrounding tissues, were explanted and excess tissue was removed. Half of the specimens (16 specimens, 8 nano-CaP and 8 GAE controls) were stored on ice for subsequent mechanical testing (torque-out). The remaining specimens for histological analysis (16 specimens, 8 nano-CaP and 8 GAE controls) were fixed in 10% neutral buffered formalin solution for further histological processing.

2.8. Mechanical testing

2.8.1. Torque testing

Torque-out values, i.e. the value necessary to remove the implant from the bone specimen, were determined using a digital torque gauge (MARK-10 Corp., New York). Then the specimens were embedded in a mold with gypsum and placed in a jig, which formed part of a tensile bench (Fig. 2). A controlled, gradually increasing rotational force (displacement 0.5 mm min^{-1}) was applied to each implant until implant loosening. The peak force measured at implant loosening was scored as the torque-out value.

Following the torque measurements the specimens were fixed in 10% neutral buffered formalin solution, dehydrated in a graded series of ethanol and embedded in methyl methacrylate (MMA). After polymerization non-decalcified longitudinal sections of the implants were prepared and stained with methylene blue and basic fuchsin and examined using a light microscope. The histological

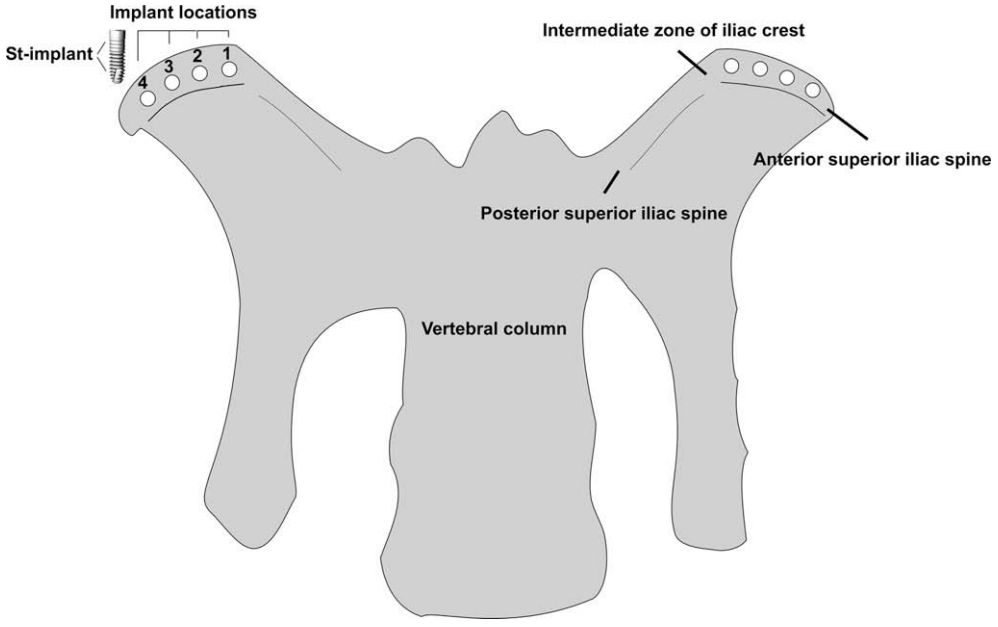

Fig. 1. Schematic representation of the pelvis of the goat. The numbered cavities represent the four implant locations in the iliac crest.

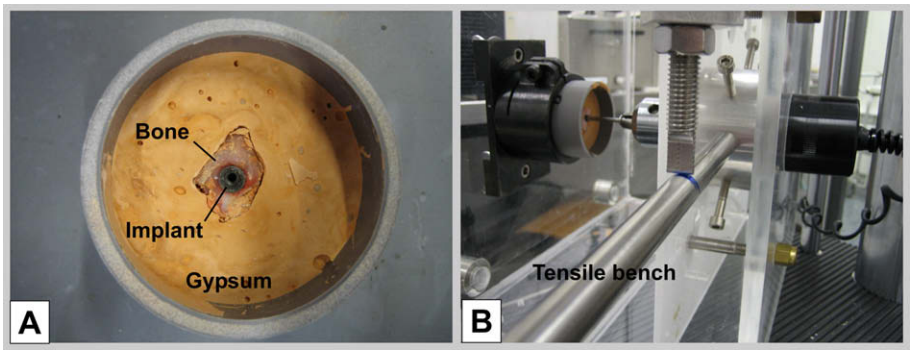

Fig. 2. Representation of the torque removal set-up. (A) After harvesting the bone specimens, containing one St implant each, were embedded in a mold with gypsum. (B) For determination of the torque-out value the mold was placed in a jig, which is part of a tensile bench. Subsequently, a controlled, gradually increasing, longitudinal force was applied via the tensile bench to each implant until it loosened. The peak force measured at implant loosening was scored as the torque-out value.

sections were examined to determine the fracture plane of the mechanically tested implants.

2.9. Histological preparations

After fixation in 10% neutral buffered formalin solution the specimens for histological processing were dehydrated gradually in ethanol solutions from 70% to 100% and subsequently embedded in MMA. Following polymerization non-decalcified 10 μm thick longitudinal sections of the implants were prepared (at least three for each implant) using a modified sawing microtome technique [33] and subsequently stained with methylene blue and basic fuchsin.

2.10. Histological and histomorphometrical evaluation

To evaluate the bone response around the implants, histological evaluation was carried out using a light microscope (Axio Imager Microscope Z1, Carl Zeiss Micro Imaging GmbH, Göttingen, Germany) equipped with a computer-based image analysis system (Leica Qwin Pro-image analysis software, Leica Imaging Systems, Cambridge, UK) to perform histomorphometrical analyses. Quantitative measurements were conducted for three different sections per specimen, on each side of the two-dimensional histological image (at magnification; 31.5×), resulting in a total of six measurements per specimen. Bone–implant contact (BC) and peri-implant bone volume (BV) were the parameters assessed. BC was calculated as the percentage of implant surface in direct contact with bone, without any fibrous tissue interposition. To determine the peri-implant BV three regions of interest (ROI) were set along the long axis of the implant for each individual sample, starting at the first coronal screw thread of the St implants (Fig. 3). The inner, middle and outer zone was marked, with a standardized length of 4000 μm and a height of 500 μm. BV was defined as the percentage of the total ROI occupied by bone tissue.

2.11. Statistical analysis

All measurements were statistically evaluated using SPSS, version 16.0 (SPSS Inc., Chicago, IL). Paired *t*-tests were used for comparison of torque-in and torque-out values for the GAE vs. nano-CaP-coated implants. Paired *t*-tests were also used to test the differences between the two experimental groups for BC, BV and the three individual BV zones (inner, middle and outer). Statistical significancy was set at a probability value of $P < 0.05$.

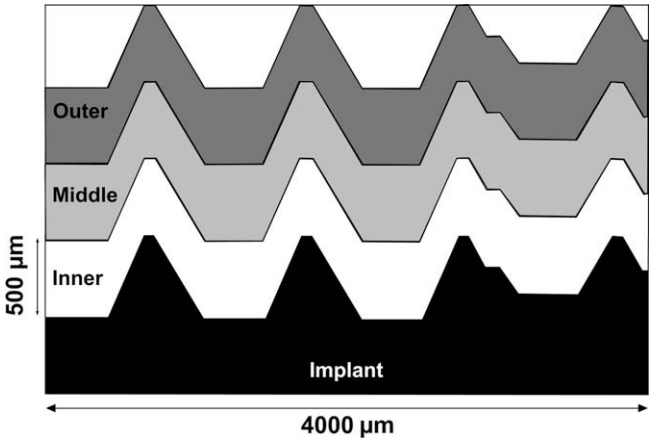

Fig. 3. Schematic representation of the quantification of bone contact (BC) and bone volume (BV) for histomorphometrical analysis. BC was calculated as the percentage of implant surface (4000 μm) which is in direct contact with bone. To determine the amount of peri-implant bone volume three ROI were set for each individual sample along the length of the implant, starting at the first coronal screw thread of the St implants. An inner, middle and outer zone were marked, with a standardized length of 4000 μm and a width of 500 μm. The peri-implant bone volume was defined as the percentage of the total area of interest in which bone was present.

3. Results

3.1. Electrosprayed coatings

3.1.1. Surface characterization

Fig. 4 displays SEM images of the GAE (Fig. 4A and B) and electrosprayed nano-CaP-coated (Fig. 4C and D) St implant surfaces. The GAE implants showed a rough surface appearance in accordance with the surface treatment. The nano-CaP coating showed a rough, porous network of densely packed nano-CaP particles distributed over the entire implant surface. At higher magnification (Fig. 4D) the nano-CaP coatings appeared to have granular depositions of different sizes on top of and in between the porous network.

The thickness of the coatings was measured using partially coated silicon wafers, which were subjected to AFM. Results obtained with AFM elucidated an electrosprayed nano-CaP coating thickness of ~400 ± 50 nm.

The results of the surface roughness measurements using UST showed an average surface roughness value (R_a) of 1.33 ± 0.01 μm for GAE surfaces and 1.28 ± 0.10 μm for nano-CaP-coated surfaces.

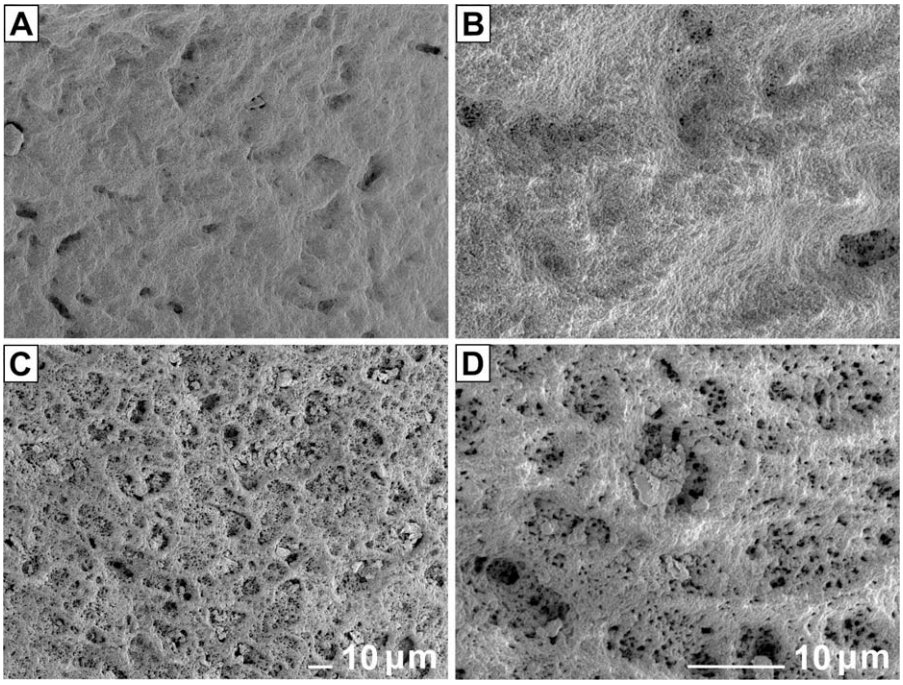

Fig. 4. SEM images of an GAE implant surface (A and B), and a nano-CaP-coated implant surface (C and D). Original magnifications: 500× (A and C); 2000× (B and D).

3.2. Implantation of St implants in artificial bone

Results obtained with the OCPC method demonstrated that 64.4 ± 4.0% of the calcium in the nano-CaP coatings remained on the implant surface after implantation in artificial bone. Furthermore, evaluation of the morphological appearance of the electrosprayed nano-CaP coatings before and after implantation in the artificial bone using SEM showed that the implant surface was still completely covered with the nano-CaP coating after implantation (data not shown).

3.3. In vivo implantation experiment

3.3.1. General observations on experimental animals

Throughout the experimental period all four goats remained in good health and did not show any post-operative wound healing complications. After 6 weeks a total of 32 implants were retrieved – all 32 St implants were still in situ (i.e. surrounded by bone). Macroscopically, the implants remained intact and no inflammatory signs or adverse tissue reactions were observed.

3.3.2. Torque testing

During removal torque testing one nano-CaP-coated St implant appeared to be loosened and was therefore excluded from the torque-out measurements. The results of the insertion (torque-in) and removal torque (torque-out) measurements for both experimental groups (GAE and nano-CaP-coated) are depicted in Fig. 5 and Table 1. Mean torque-in values were 32.1 and 32.8 N cm^{-1} for the GAE and nano-CaP-coated implants, respectively. Mean torque-out values after 6 weeks implantation were 42.8 and 36.8 N cm^{-1} for the GAE and nano-CaP-coated implants, respectively. Regarding the mean difference in torque-in values for the two experimental groups, no significant differences were observed. Similarly, no significant differences were observed for the torque-out values for the GAE and nano-CaP-coated groups. Additionally, the torque-in and torque-out values for each

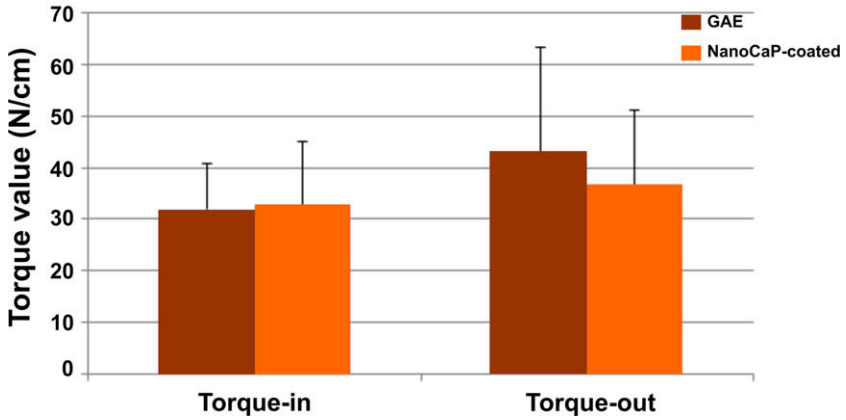

Fig. 5. Results of the torque testing showing mean values ± SD (N cm^{-1}) for both experimental groups for insertion (torque-in) and removal (torque-out) torque values.

Table 1
Mean values ± SD (N cm^{-1}) and the outcome of the statistical analyses for both experimental groups regarding insertion (torque-in) and removal (torque-out) torque values.

	GAE	Nano-CaP-coated	*P* value
Torque-in	32.06 ± 8.85	32.77 ± 12.37	0.90
Torque-out	42.80 ± 20.87	36.81[a] ± 14.62	0.54

[a] One nano-CaP-coated implant appeared to be loosened upon removal torque testing and was therefore excluded from the analysis.

individual group were analyzed and also did not show significant differences.

Light microscopic examination of the fracture plane of specimens subjected to torque testing showed similar results for the GAE and nano-CaP-coated implants. After 6 weeks implantation the fracture plane was observed to be located at the implant–coating interface (Fig. 6).

3.3.3. Descriptive histological evaluation

Light microscopic examination of methylene blue/basic fuchsin stained sections of the retrieved specimens demonstrated variable amounts of bone inside and on top of the threads of the St implants (Fig. 7). All implants were inserted for the major part into trabecular bone. No apparent differences between the two experimental groups were observed. On more detailed observation it was observed that generally for all St implants, irrespective of surface modification, the peripheral pitch of the threads was in close contact with the surrounding bone tissue. Moreover, it was observed that the bone present in the pitch was conducted along the implant surface into the threads. A striking observation in various sections was the presence of a cartilaginous growth plate at the top of the iliac crest, from which in some cases an intervening fibrous tissue layer was present along the implant surface.

3.3.4. Histomorphometrical analysis

Mean data regarding BC and BV and the outcome of statistical analyses between the experimental groups for the three peri-implant zones (inner, middle and outer) are depicted in Fig. 8 and Table 2.

3.3.4.1. Bone contact. Overall data for bone–implant contact did not show significant differences between the GAE (23.2%) and nano-CaP-coated group (23.0%) groups (Fig. 8A).

3.3.4.2. Bone volume. Regarding overall bone volume, no significant differences were observed between the GAE (40.9%) and nano-CaP-coated (38.8%) groups (Fig. 8B). Additionally, the bone volume values for the different peri-implant zones (inner, middle and outer) showed no significant differences between the GAE (43.3%, 42.1% and 37.5%) and nano-CaP-coated (41.5%, 38.6% and 36.2%) groups.

4. Discussion

The current study was initiated to evaluate the mechanical properties and the in vivo bone response to electrosprayed nano-CaP-coated implants compared with GAE implant surfaces, using the iliac crest of goats as an implantation model. The results of the present study show that electrosprayed nano-CaP coatings perform to a comparable extent to GAE implants, both with respect to implant fixation and bone healing response.

4.1. Coating properties

The electrospray deposition technique, as used for the deposition of nano-CaP coatings in the present study, is a so-called line-of-sight deposition technique. For deposition and characterization of the coatings on the dental implants used in the present study several practical issues are involved. First, determination of coating thickness directly on the implant surface was impossible due to (i) the pre-existing surface roughness resulting from the grit blasting and acid etching procedure, (ii) the three-dimensional configuration of the implants and (iii) the presence of screw threads on the implant surface. Consequently, coating thickness was determined using a validated model system (unpublished results) in which planar silicon

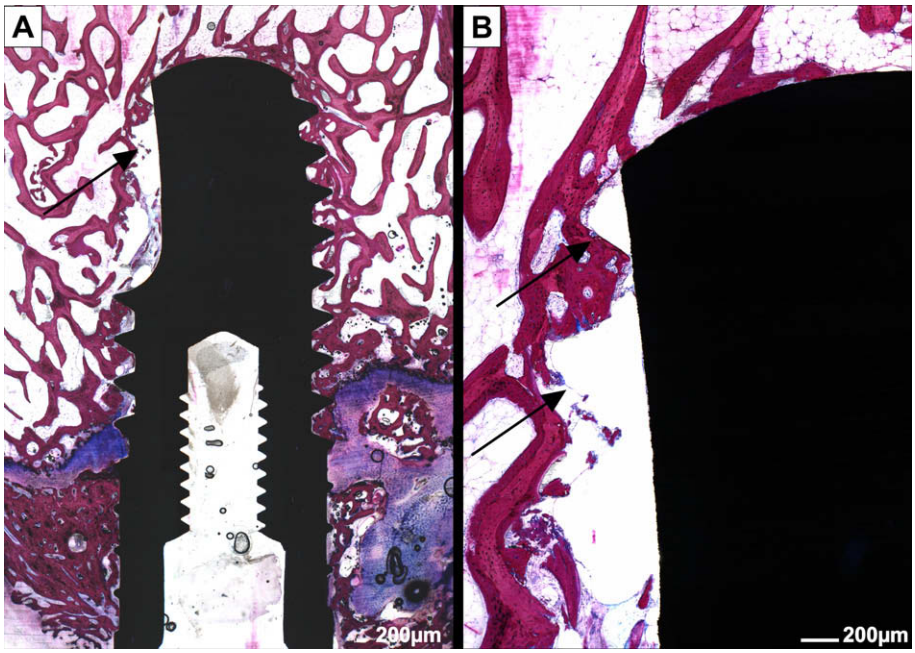

Fig. 6. Histological sections of a screw-type (St) implant coated with a nano-CaP-coating after mechanical torque testing (A and B). After 6 weeks implantation the fracture plane was observed to be located at the implant–coating interface (see arrows). Magnification: (A) 31,5×; (B) 126×.

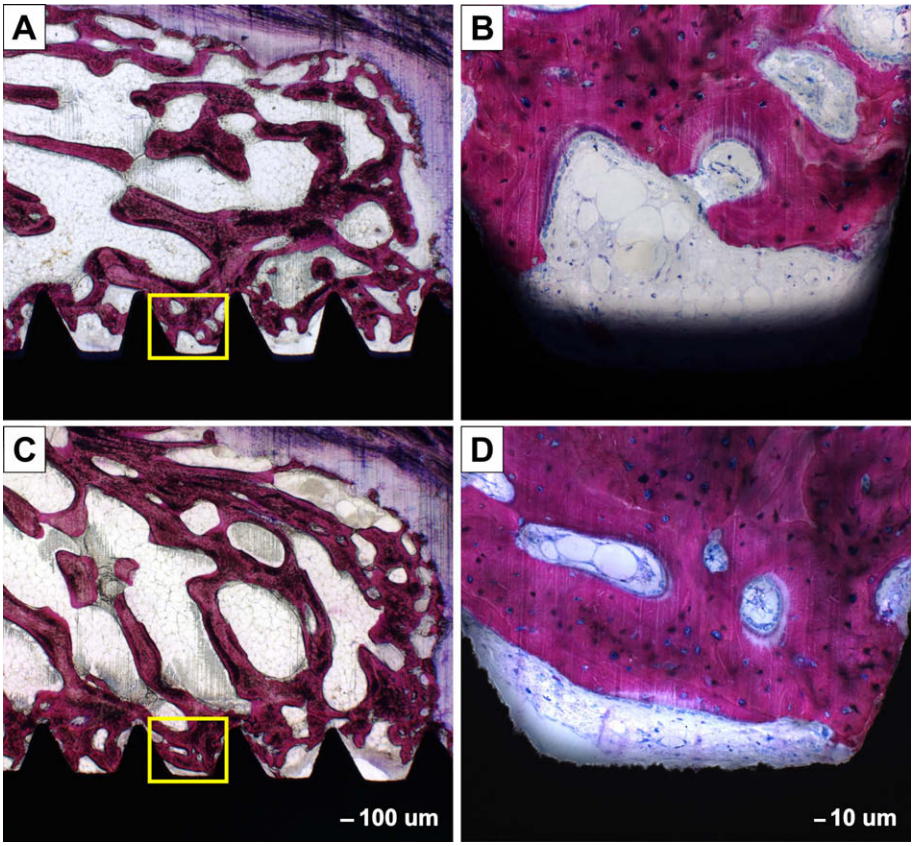

Fig. 7. Representative histological sections of St implants after 6 weeks implantation in the crista iliaca of goats. (A and B) GAE; (C and D) nano-CaP-coated implants. Magnification: (A and C) 31,5×; (B and D) 126×.

wafers serve as model substrates for coating deposition. Second, complete surface coverage of a three-dimensional dental implant by the electrospray deposition technique can only be achieved by either continuous rotation of the implant during coating deposition or performing multiple coating deposition runs, as in the present study. Although the authors are aware of the fact that the option of continuous rotation of the implant during coating deposition is preferable for homogeneous coating thickness over the entire implant surface, the experimental set-up of the electrospray equipment lacks a rotational implant holder. Consequently, the dental implants were coated in two runs that resulted in complete surface coverage by nano-CaP, as was seen by electron microscopy.

4.2. Mechanical testing

Torque-out tests determine the force that is needed to loosen implants from their surrounding bone, which is indicative of the bone–implant interface strength [34]. The present study showed similar mean torque values for the nano-CaP-coated and GAE implants, with high variation (i.e. standard deviation) within each individual group. The high intra-group variation most likely resulted from variations in implant location within the iliac crest, used for reasons of statistical randomization. It is straightforward to hypothesize that in this way location-dependent effects are minimized, albeit that variations in torque values increase due to slight differences in the anatomical surrounding of the implants. From a mechanical point of view this lack of difference can be explained by the comparable surface roughness values for both experimental groups ($R_a \approx 1.3$ μm). However, in addition to surface roughness, surface composition plays a major role in obtaining an optimal bone–implant interface [35,36]. Surprisingly, addition of the nano-CaP coating did not result in an improvement in bone bonding. The reasons for this lack of a beneficial effect of the nano-CaP could be multiple. Outsiders might speculate that detachment of the coating upon insertion is a likely cause. However, indirect evidence exists that contradicts such speculations. Several studies showed that thin nano-sized CaP coatings, up to 400 nm, mainly consist of poorly crystalline particles [28,37,38]. As coating crystallinity and mechanical strength are positively related, nanometer thin electrosprayed CaP coatings need a certain degree of crystallinity in order to ensure interfacial adhesion to the substrate and sufficient mechanical strength of the applied coating upon implantation [39]. However, as shown in the assay using artificial bone, the nanometer thin CaP coatings did show sufficient adhesion strength to withstand the shear and compressive forces upon implantation, as expressed by a coating retention of ~64%. Another speculative reason for the lack of an additional favorable effect of the nano-CaP coating might be fast dissolution of the coating. It has been reported by Wolke et al. that the dissolution behavior of coatings is determined by the degree of coating crystallinity, i.e. a lower degree of crystallinity causes a higher dissolution rate [40]. In view of this, it can be hypothesized that in the current study dissolution of the coating occurred before it had a chance to influence the bone healing response. Dissolution of CaP ceramic coatings can be enhanced by the local bone conditions after creation of the wound bed, which is associated with a decrease in pH [40]. In view of this, coating dissolution as a possible cause for the lack of a significant effect cannot be ruled out and needs to be addressed in future experimental work on electrosprayed nano-CaP coatings. A final explanation might be that, within the context of the experimental model used, addition of the nano-CaP coating could not improve the already

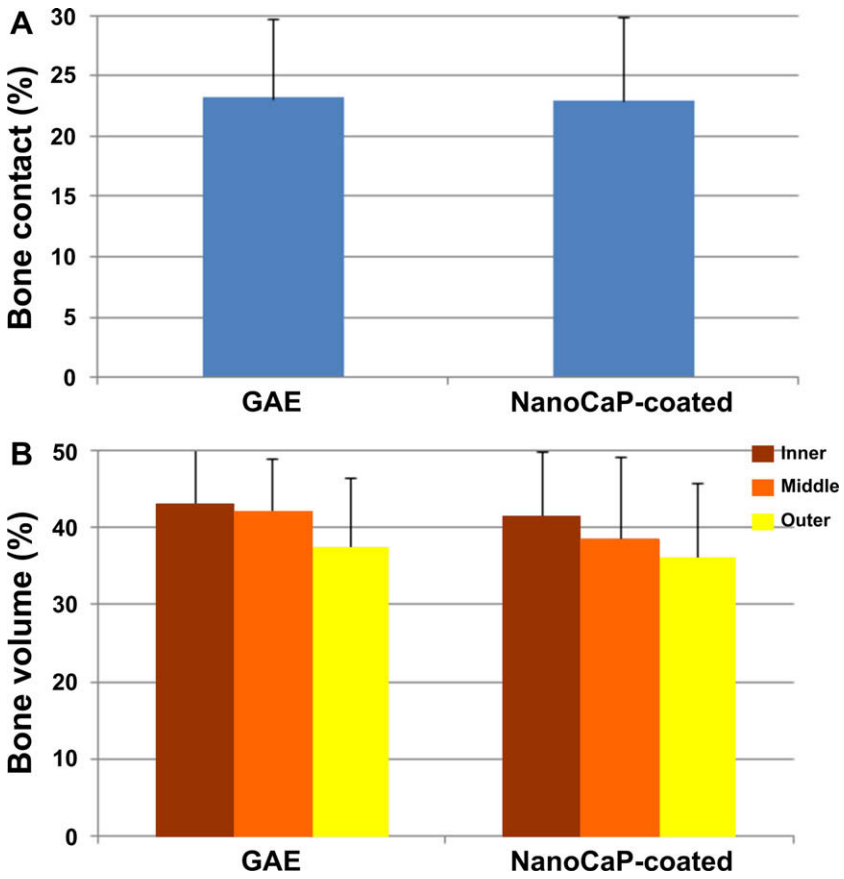

Fig. 8. Results of histomorphometrical analyses of St implants inserted in the crista iliaca of goats. Bone × implant contact (A) and bone volume values (B), specified for the three different peri-implant zones (inner, middle and outer) after 6 weeks implantation are shown for both experimental groups (GAE and nano-CaP-coated). No interaction between the experimental groups and different peri-implant zones were found.

Table 2
Mean, mean difference ± SD and the outcome of the statistical analyses for the variables bone contact (BC), bone volume (BV) and the different peri-implant zones (inner, middle and outer).

		Histomorphometry		
		Mean	Mean difference	*P* value
Overall bone contact	GAE	23.16 ± 6.58	0.16 ± 6.87	0.95
	Nano-CaP-coated	23.00 ± 6.89		
Overall bone volume	GAE	40.93 ± 7.93	2.16 ± 6.25	0.36
	Nano-CaP-coated	38.77 ± 8.71		
Bone volume				
Inner	GAE	43.30 ± 9.15	1.76 ± 6.92	0.50
	Nano-CaP-coated	41.50 ± 7.06		
Middle	GAE	42.10 ± 8.41	3.45 ± 9.64	0.35
	Nano-CaP-coated	38.60 ± 10.79		
Outer	GAE	37.50 ± 9.14	1.26 ± 8.63	0.69
	Nano-CaP-coated	36.20 ± 9.58		

excellent biological effect induced by a GAE surface alone. This phenomenon will be thoroughly addressed in the next paragraph.

4.3. In vivo evaluation

With respect to bone contact and bone volume, no significant differences were found for the GAE and nano-CaP-coated implants after 6 weeks implantation in the iliac crest. These results indicate that electrosprayed nano-CaP coatings are able to improve the bone response to a comparable extent to the GAE control implants. Evidently, adding a nano-CaP coating has, within the restrictions of this experimental model, no additional value.

The beneficial effect on peri-implant bone formation of calcium phosphate coatings on titanium implants has been confirmed in numerous studies [12,22]. To overcome drawbacks, such as delamination of coating fragments resulting in failure of the implant [41–43], the electrostatic spray deposition technique was introduced, which allows the production of nanometer thin coatings [28,44,45].

The results obtained in the present study have demonstrated that the addition of a nanometer thin CaP coating did not significantly enhance bone healing around St implants compared with GAE implant surfaces. This observation corroborates published data comparing acid-etched surfaces with CaP-coated surfaces [46] and GAE surfaces with CaP-coated surfaces [47]. In contrast to these findings, a recently published study by Schouten et al. demonstrated that when using an intramedullary gap healing model, the presence of a nano-CaP coating significantly improved bone–implant contact after 4 weeks implantation compared with GAE surfaces [45]. This biological response proves that nano-CaP coatings are able to enhance the osteogenic response in cases of non-intimate bone–implant contact.

The authors hypothesize that these contradictory results are due to the applied study design. In the current study the St implants (diameter 4.2 mm) were inserted into a pre-drilled cavity measuring 4.0 mm in diameter, according to the manufacturer's instructions. Using this press fit surgical approach small bone fragments are loosened due to shear forces at the bone–implant interface and subsequently pressed in between the trabecular voids and screw threads during implant placement. As a result of this

translocation of bone fragments new peri-implant bone formation is initiated and implant stability enhanced [48,49]. The intimate bone contact achieved by the press fit surgical approach in this study apparently overshadowed the effect of the nano-CaP coating. This is in contradiction to compromised situations in which imperfect implant–tissue contact is obtained upon implantation. The latter was shown by Conner et al., who showed in a canine model that hydroxyapatite-coated implants significantly enhanced bone contact compared with acid-etched surfaces in the case of a non-intimate bone–implant contact (gap 2 mm), whereas no significant differences were observed in the case of intimate bone–implant contact at the time of implant placement [46].

5. Conclusion

The present study has demonstrated that electrosprayed nano-CaP coatings evoke a similar bone response to GAE implants in the case of press fit implant placement. Also, equal torque values were observed for the two experimental groups. The authors hypothesize that the previously demonstrated additional effect of nano-CaP coating was overshadowed by the optimal peri-implant osseous environment in the present experiment, created by the press fit surgical approach.

Acknowledgements

The authors acknowledge Dr. E.M. Bronkhorst for his assistance with the statistical analysis, Mr. V. Cuijpers for his assistance with the histomorphometrical analysis and Ms. N. van Dijk for her assistance with the histological sectioning. Additionally, the authors thank Dyna Dental Engineering BV (Bergen op Zoom, The Netherlands) for providing the implants and the Dutch Program for Tissue Engineering for their financial support (NGT.6730).

Appendix A. Figures with essential colour discrimination

Certain figure in this article, particularly Figures 2, 5–8, is difficult to interpret in black and white. The full colour images can be found in the on-line version, at doi: 10.1016/j.actbio.2009.11.030.

References

[1] Brunski JB, Puleo DA, Nanci A. Biomaterials and biomechanics of oral and maxillofacial implants: current status and future developments. Int J Oral Maxillofac Implants 2000;15(1):15–46.
[2] Siebers MC, Ter Brugge PJ, Walboomers XF, Jansen JA. Integrins as linker proteins between osteoblasts and bone replacing materials. A critical review. Biomaterials 2005;26(2):137–46.
[3] Puleo DA. Implant surfaces. Dental Clin N Am 2006;50(3):323–38.
[4] Buser D, Schenk RK, Steinemann S, Fiorellini JP, Fox CH, Stich H. Influence of surface characteristics on bone integration of titanium implants. A histomorphometric study in miniature pigs. J Biomed Mater Res 1991;25(7):889–902.
[5] Gotfredsen K, Berglundh T, Lindhe J. Anchorage of titanium implants with different surface characteristics: an experimental study in rabbits. Clin Implant Dent Relat Res 2000;2(3):120–8.
[6] Wennerberg A, Albrektsson T, Lausmaa J. Torque and histomorphometric evaluation of c.p. titanium screws blasted with 25- and 75-μm-sized particles of Al_2O_3. J Biomed Mater Res 1996;30(2):251–60.
[7] Abrahamsson I, Berglundh T, Linder E, Lang NP, Lindhe J. Early bone formation adjacent to rough and turned endosseous implant surfaces – an experimental study in the dog. Clin Oral Implants Res 2004;15(4):381–92.
[8] Cochran DL, Schenk RK, Lussi A, Higginbottom FL, Buser D. Bone response to unloaded and loaded titanium implants with a sandblasted and acid-etched surface: a histometric study in the canine mandible. J Biomed Mater Res 1998;40(1):1–11.
[9] Wennerberg A, Albrektsson T, Johansson C, Andersson B. Experimental study of turned and grit-blasted screw-shaped implants with special emphasis on effects of blasting material and surface topography. Biomaterials 1996;17(1):15–22.
[10] Wennerberg A, Hallgren C, Johansson C, Danelli S. A histomorphometric evaluation of screw-shaped implants each prepared with two surface roughnesses. Clin Oral Implants Res 1998;9(1):11–9.
[11] de Jonge LT, Leeuwenburgh SCG, Wolke JGC, Jansen JA. Organic–inorganic surface modifications for titanium implant surfaces. Pharm Res 2008;25(10):2357–69.
[12] Dhert WJA. Retrieval studies on calcium phosphate-coated implants. Med Prog Technol 1994;20(3–4):143–54.
[13] Dorozhkin SV, Epple M. Biological and medical significance of calcium phosphates. Angew Chem Int Ed 2002;41(17):3130–46.
[14] Lacefield WR. Materials characteristics of uncoated/ceramic-coated implant materials. Adv Dent Res 1999;13:21–6.
[15] de Groot K, Geesink R, Klein CP, Serekian P. Plasma sprayed coatings of hydroxylapatite. J Biomed Mater Res 1987;21(12):1375–81.
[16] Geesink RGT, Degroot K, Klein CPAT. Chemical implant fixation using hydroxyl-apatite coatings – the development of a human total hip-prosthesis for chemical fixation to bone using hydroxyl-apatite coatings on titanium substrates. Clin Orthop Relat Res 1987(225):147–70.
[17] Soballe K, Hansen ES, Brockstedtrasmussen H, Bunger C. Hydroxyapatite coating converts fibrous tissue to bone around loaded implants. J Bone Joint Surg Br Vol 1993;75(2):270–8.
[18] Caulier H, Vanderwaerden JPCM, Paquay YCGJ, Wolke JGC, Kalk W, Naert I, et al. Effect of calcium–phosphate (Ca–P) coatings on trabecular bone response – a histological study. J Biomed Mater Res 1995;29(9):1061–9.
[19] Schouten C, Meijer GJ, van den Beucken JJJP, Spauwen PHM, Jansen JA. Effects of implant geometry, surface properties and TGF-b1 on peri-implant bone response: an experimental study in goats. Clin Oral Implants Res 2008;20(4):421–9.
[20] Clemens JAM, Klein CPAT, Sakkers RJB, Dhert WJA, Degroot K, Rozing PM. Healing of gaps around calcium phosphate-coated implants in trabecular bone of the goat. J Biomed Mater Res 1997;36(1):55–64.
[21] Manders PJD, Wolke JGC, Jansen JA. Bone response adjacent to calcium phosphate electrostatic spray deposition coated implants: an experimental study in goats. Clin Oral Implants Res 2006;17(5):548–53.
[22] de Groot K, Wolke JGC, Jansen JA. Calcium phosphate coatings for medical implants. Proc Inst Mech Eng H 1998;212(H2):137–47.
[23] Geesink RGT. Osteoconductive coatings for total joint arthroplasty. Clin Orthop Relat Res 2002(395):53–65.
[24] Hulshoff JEG, Jansen JA. Initial interfacial healing events around calcium phosphate (Ca–P) coated oral implants. Clin Oral Implants Res 1997;8(5):393–400.
[25] Jansen JA, Vandewaerden JPCM, Wolke JGC, Degroot K. Histologic evaluation of the osseous adaptation to titanium and hydroxyapatite-coated titanium implants. J Biomed Mater Res 1991;25(8):973–89.
[26] Morozov VN, Morozova TY. Electrospray deposition as a method to fabricate functionally active protein films. Anal Chem 1999;71(7):1415–20.
[27] Webster TJ, Ergun C, Doremus RH, Siegel RW, Bizios R. Enhanced osteoclast-like cell functions on nanophase ceramics. Biomaterials 2001;22(11):1327–33.
[28] de Jonge LT, Leeuwenburgh S, van den Beucken JJJP, te Riet J, Daamen WF, Wolke JGC, et al. Electrosprayed nanometer-thick collagen/calcium phosphate coatings for improved mechanical and biological performance of titanium implants. Biomaterials, accepted for publication..
[29] Cai YR, Liu YK, Yan WQ, Hu QH, Tao JH, Zhang M, et al. Role of hydroxyapatite nanoparticle size in bone cell proliferation. J Mater Chem 2007;17(36):3780–7.
[30] Shi ZL, Huang X, Cai YR, Tang RK, Yang DS. Size effect of hydroxyapatite nanoparticles on proliferation and apoptosis of osteoblast-like cells. Acta Biomater 2009;5(1):338–45.
[31] de Jonge LT, van den Beucken JJJP, Leeuwenburgh S, Hamers A, Wolke J, Jansen JA. In vitro responses to electrosprayed alkaline phosphatase/calcium phosphate composite coatings. Acta Biomater 2009;5(7):2773–82.
[32] Schouten C, Meijer GJ, Beucken JJJP, Spauwen PHM, Jansen JA. A novel implantation model for evaluation of the bone healing response to dental implants: the goat iliac crest. Clin Oral Implants Res, accepted for publication..
[33] van der Lubbe HB, Klein CP, de Groot K. A simple method for preparing thin (10 microM) histological sections of undecalcified plastic embedded bone with implants. Stain Technol 1988;63(3):171–6.
[34] An YH, Draughn RA. Mechanical testing of bone and the bone–implant interface. New York: CRC Press; 2000. p. 489–96.
[35] Boyan BD, Hummert TW, Dean DD, Schwartz Z. Role of material surfaces in regulating bone and cartilage cell response. Biomaterials 1996;17(2):137–46.
[36] Schwartz Z, Boyan BD. Underlying mechanisms at the bone–biomaterial interface. J Cell Biochem 1994;56(3):340–7.
[37] Fernandez-Pradas JM, Cleries L, Martinez E, Sardin G, Esteve J, Morenza JL. Influence of thickness on the properties of hydroxyapatite coatings deposited by KrF laser ablation. Biomaterials 2001;22(15):2171–5.
[38] Fernandez-Pradas JM, Cleries L, Sardin G, Morenza JL. Characterization of calcium phosphate coatings deposited by Nd:YAG laser ablation at 355 nm: influence of thickness. Biomaterials 2002;23(9):1989–94.
[39] Leeuwenburgh SCG, Wolke JGC, Lommen L, Pooters T, Schoonman J, Jansen JA. Mechanical properties of porous, electrosprayed calcium phosphate coatings. J Biomed Mater Res A 2006;78A(3):558–69.
[40] Wolke JGC, de Groot K, Jansen JA. In vivo dissolution behavior of various RF magnetron sputtered Ca–P coatings. J Biomed Mater Res 1998;39(4):524–30.
[41] Goodman SB, Lind M, Song Y, Smith RL. In vitro, in vivo, and tissue retrieval studies on particulate debris. Clin Orthop Relat Res 1998(352):25–34.
[42] Gross KA, Ray N, Rokkum M. The contribution of coating microstructure to degradation and particle release in hydroxyapatite coated prostheses. J Biomed Mater Res 2002;63(2):106–14.

[43] Munting E, Wilmart JF, Wijne A, Hennebert P, Delloye C. Effect of sterilization on osteoinduction. Comparison of five methods in demineralized rat bone. Acta Orthop Scand 1988;59(1):34–8.
[44] Mendonca G, Mendonca DBS, Aragao FJL, Cooper LF. Advancing dental implant surface technology – from micron- to nanotopography. Biomaterials 2008;29(28):3822–35.
[45] Schouten C, van den Beucken JJJP, de Jonge LT, Bronkhorst EM, Meijer GJ, Spauwen PHM, et al. The effect of alkaline phosphatase coated onto titanium alloys on bone responses in rats. Biomaterials 2009;30(32):6407–17.
[46] Conner KA, Sabatini R, Mealey BL, Takacs VJ, Mills MP, Cochran DL. Guided bone regeneration around titanium plasma-sprayed, acid-etched, and hydroxyapatite-coated implants in the canine model. J Periodontol 2003;74(5):658–68.
[47] He FM, Yang GL, Wang XX, Zhao SF. Bone responses to rough titanium implants coated with biomimetic Ca–P in rabbit tibia. J Biomed Mater Res B 2009;90B(2):857–63.
[48] O'Sullivan D, Sennerby L, Meredith N. Influence of implant taper on the primary and secondary stability of osseointegrated titanium implants. Clin Oral Implants Res 2004;15(4):474–80.
[49] Shalabi MM, Wolke JGC, Jansen JA. The effects of implant surface roughness and surgical technique on implant fixation in an in vitro model. Clin Oral Implants Res 2006;17(2):172–8.